Highly elastomeric poly(3-hydroxyoctanoate) based natural polymer composite for enhanced keratinocyte regeneration

Rai, Ranjana ; Roether, Judith A ; Knowles, Jonathan C ; Mordan, Nicola ; Salih, Vehid ; Locke, Ian C ; Gordge, Michael P ; McCormick, Aine ; Mohn, Dirk ; Stark, Wendelin J ; Keshavarz, Tajalli ; Boccaccini, Aldo R ; Roy, Ipsita

DOI: https://doi.org/10.1080/00914037.2016.1217530

Highly elastomeric Poly(3-hydroxyoctanoate) based natural polymer composite for enhanced keratinocyte regeneration

Ranjana Rai[a], Judith A. Roether[b], Jonathan C. Knowles[c,d], Nicola Mordan[c], Vehid Salih[c], Ian C. Locke[e], Michael P. Gordge[e], Aine.Mc Cormick[f], Dirk Mohn[g,h], Wendelin J. Stark[g], Tajalli Keshavarz[a], Aldo R. Boccaccini[b] and Ipsita Roy[a]**

[a]*Department of Life Sciences, Faculty of Science and Technology, University of Westminster, London W1W 6UW, UK*
[b]*Department of Materials Science and Engineering, University of Erlangen – Nuremberg Cauestr. 6., 91058 Erlangen, Germany.*
[c]*Division of Biomaterials and Tissue Engineering, UCL Eastman Dental Institute, University College London, 256 Grays Inn Road, London WCIX 8LD, UK*
[d]*WCU Research Centre of Nanobiomedical Science, Dankook University, San#29, Anseo-dong, Dongnam-gu, Cheonan-si, Chungnam, 330-714, South Korea*
[e]*Department of Biomedical Sciences, Faculty of Science and Technology, University of Westminster, London W1W 6UW, UK*
[f]*Haemophilia Reference Centre, St. Thomas' Hospital , Lambeth Palace Road, London SE1 7EH, UK*
[g]*Institute for Chemical and Bioengineering, Department of Chemistry and Applied Biosciences, ETH Zurich, 8093 Zurich, Switzerland*
[h]*Department of Preventive Dentistry, Periodontology, and Cariology, University of Zurich Center of Dental Medicine, 8032 Zurich, Switzerland*

***Corresponding authors**
Professor Ipsita Roy
Department of Life Sciences
Faculty of Science and Technology,
University of Westminster
London W1W 6UW
Phone no: +44-2079115000 ext 3567
Fax: +44-2079115087
email: royi@wmin.ac.uk

Professor A.R. Boccaccini
Department of Materials Science and Engineering,
University of Erlangen – Nuremberg
Cauestr. 6., 91058 Erlangen, Germany
Phone no: +49 9131 85 28601
Fax: +49 9131 85 28602
email: aldo.boccaccin@ww.uni-erlangen.de

Abstract

A novel nanocomposite material which combines the biocompatible, elastomeric, natural, biodegradable homopolymer, poly(3-hydroxyoctanoate), P(3HO), with haemostatic and antibacterial bioactive glass nanoparticles (n-BG), were developed as a matrix for skin related applications. P(3HO) is a unique member of the family of natural polyhydroxyalkanoate biopolymers. The P(3HO)/n-BG composite films were fabricated using the solvent casting method. Microstructural studies revealed n-BG particles both embedded in the matrix and deposited on the surface which introduced nanotopography and increased its hydrophilicity. The composite exhibited an increase in the Young's modulus when compared to the control, yet maintained flexible elastomeric properties. These changes in the surface topography and chemistry of the composite system led to an increase of protein adsorption and cytocompatibility for the seeded human keratinocyte cell line (HaCaT). The results from this study demonstrated that the fabricated P(3HO)/n-BG composite system is a promising novel matrix material with potential applications in skin tissue engineering and wound healing.

Key words: Poly(3-hydroxyoctanoate), bioactive glass, composites, skin tissue engineering, wound healing

1. Introduction

The skin is the largest organ in humans, acting as a protective interphase between the human body and the surrounding, which protects underlying organs and also plays a pivotal role in fluid homeostasis, sensory detection and self-healing.[1-4] When the structural integrity of the skin is damaged or lost, impairment of the skin functions occur resulting in minor to significant disability and may even lead to death.[4-7] Such large skin defects therefore require immediate intervention to protect the wound from infections and to replace the damaged and lost skin.[8] Autografts and allografts have been conventionally used to treat burns and other full thickness wounds. For dermal wound healing use of autografts is a "gold standard" as no immune rejection is encountered.[9] However, this approach suffers from limited availability and the risk of donor site morbidity. Allografts, though not limited by availability, pose risks of disease transmission and immune rejections.[10-13]

A wide range of research is now being undertaken on the development and clinical use of tissue engineered skin grafts to overcome the limitation of autografts and allografts. In this tissue engineering approach, the relevant skin cells are seeded and populated in a suitable matrix designed to mimic the skin's natural extracellular matrix (ECM) with or without the use of additional chemical cues. The skin cell matrix construct is then grafted on to the wound (epidermal graft); cells then proliferate from the matrix to the wound bed forming cell clusters and ultimately the normal epidermis.[14, 15] The matrix thus provides healthy replacement cells, protection to the wound, until it is degraded or absorbed [14, 15], and elasticity and mechanical support to the regenerating skin. Amongst the natural materials, one promising candidate for designing the matrix support, are the polyhydroxyalkanoate (PHA) family of biopolymers [16] PHAs are polyesters of 3-hydroxyacids biosynthesized from bacteria using a variety of carbon sources.[17] The PHAs may be short chain length (scl), containing C_3 to C_5 carbon atoms or medium chain length (mcl) containing C_6 to C_{14} carbon atoms in the monomer units. PHAs

are a highly promising family of biodegradable biomaterials, yet to be extensively used for biomedical applications. They have a wide range of chemical structures leading to mechanical properties ranging from hard and brittle to soft and elastomeric, suitable for various tissue engineering (TE) applications.[18] Their degradation products are much less acidic than those of Polylactic acid, PLA and Poly(lactic-co-glycolic acid), PLGA, leading to higher biocompatibility. Also, their degradation occurs by surface degradation, as opposed to the bulk degradation of PLA or PLGA, leading to highly controlled degradation, highly desirable for TE applications.

In this work we have used a novel homopolymer, poly(3-hydroxyoctanoic acid), P(3HO), an mcl-PHA, which is unique and has been produced and described for the first time by Rai *et al.*[19] The P(3HO) is biosynthesized using the bacteria *P. mendocina* grown on an octanoate feed.[19] The polymer P(3HO) has promising properties of flexible elastomeric nature and biocompatibility amenable for soft tissue engineering such as skin tissue engineering.[20] The highly flexible nature of P(3HO) would enable its application into wound beds located in difficult contours of the body and also sustain and recover from multiple deformations without adversely affecting the surrounding tissues. Additionally, due to its biodegradable nature, P(3HO) would provide a temporary mechanical support for the healthy cells without additional surgical intervention for its subsequent removal.

However, PHAs, including P(3HO), are relatively hydrophobic in nature and are not as highly bioactive.[21] In recent years numerous studies have been carried out to study the cumulative effect of combining an inorganic phase with biodegradable polymers to develop composite systems.[22] Bioactive glasses have been shown to form tenacious bonds to both hard and soft tissues; bonding is enabled by the formation of a hydroxyapatite (similar to biological apatite) layer on the glass surface on exposure to biological fluids both *in vitro* and *in vivo*.[23, 24] Incorporation of such bioactive glasses into polymer matrices improves the hydrophilicity [25,

[26] and also allows tailorability of the mechanical properties and degradation kinetics of the composite systems to match with the regenerative rate of the target tissue.[22] Bioactive glasses being bactericidal [27] are particularly important as one of the major challenges in healing chronic wound is the prevention of infection from opportunistic pathogens.[28] Bioactive glasses have also been reported to support angiogenesis which is crucial for stimulating neovascularisation of tissue engineered constructs.[29, 30] Furthermore, mesoporous bioactive glass particles have also exhibited haemostatic activity under *in vitro* conditions.[31]

Although bioactive glasses (microsize and nanosize), especially Bioglass®, have been incorporated into PHAs, these have been mainly scl-PHAs, in order to develop composites with focus on bone tissue engineering and drug delivery applications.[25, 32] In this study therefore we sought to investigate, for the first time, the potential of a novel nanocomposite system of poly(3-hydroxyoctanoate), a promising new biodegradable and biocompatible natural polymer, with bioactive glass nanoparticles (nBG) as a unique matrix support for skin tissue engineering applications.

2. Materials and Methods

2.1. Materials

The homopolymer poly(3-hydroxyoctanoate), P(3HO), used in this study was biosynthesized using *P. mendocina* grown in octanoate feed.[19] The bioactive glass particles (n-BG) used were of nanosize (average diameter, ~30 nm) with the following composition in wt% : SiO_2, 46.08 % ; Na_2O, 2.96 % ; CaO, 28.18 % and P_2O_5, 3.77 %.[25] The fabrication of these nanoparticles by flame spray synthesis and the physical characterisation has been presented by Brunner *et al*.[33]

2.2. Fabrication of films

Fabrications of the films were carried out using the solvent casting method. For the fabrication of the P(3HO) neat films (control), 5 and 10 wt % of the polymer was thoroughly dissolved in 10 mL of $CHCl_3$. The polymer solution was then filtered and cast into glass petri dishes (40 mm diameter). The films were then left to air dry at room temperature for 1 week followed by freeze drying for 10 days. These P(3HO) neat films will be referred as 5 wt% neat and 10 wt% neat.

For the fabrication of the P(3HO)/n-BG composite films, 1 wt % of n-BG was added to the filtered 5 wt% and 10 wt% polymer solutions corresponding to a n-BG concentration of 17 % v/v and 9 % v/v respectively. The polymer/n-BG mixtures were then sonicated using a sonicator (Philip Harris Scientific) at a pulse rate of 2 pulses/sec for a period ranging between 1 and 2 minutes. The composite films were then cast and prepared similarly like that of the control films. These composite films were referred to as 5 wt% and 10 wt % composite.

2.3. Microstructural studies

2.3.1. Scanning electron microscopy (SEM)

Microstructural studies for the surface topography were carried out using a JEOL 5610LV scanning electron microscope. The samples were placed on 8 mm diameter aluminium stubs and then sputter coated with gold using an EMITECH-K550 sputtering device. An operating pressure of 7 x 10^{-2} bar and deposition current of 20 mA for 2 minutes were used. SEM images were taken with an acceleration voltage of 15 kV (maximum) to avoid incineration of the polymer due to the beam heat.

2.3.2. White light interferometry study (Zygo®)

White light interferometry was used to obtain 3D images of the surface topography of samples by means of the analyzer Zygo® (New View 200 OMP 0407C). This measurement

allowed the quantification of the roughness and also a visual investigation of the topography of the surfaces.

2.3.3. Contact angle study

Static contact angle measurements were carried out to evaluate the wettability i.e. hydrophilicity of the fabricated films. A gas tight micro syringe was used to place an equal volume of water (<10 μl) on every sample by means of forming a drop. Photos (frame interval of 1 second, number of frames = 100) were taken to record the shape of the drops. Water contact angles on the specimens were measured by analysing the recorded drop images using the Windows based KSV CAM software. Four repeats for each sample were carried out. The experiment was done on a KSV CAM 200 optical contact angle meter (KSV Instruments Ltd).

2.4. Mechanical properties

Tensile testing was performed using a Perkin–Elmer dynamic mechanical analyzer at room temperature. Sample strips (N=6) were of 10 mm length and 4 mm width, cut from the solvent cast films. The initial load was set to 1 mN and then increased to 6000 mN at the rate of 200 mN min^{-1}. Young's modulus, stress and strain were recorded during the test.

2.5. Thermal properties

The thermal properties of the fabricated materials, i.e. glass transition temperature (T_g) and melting temperature (T_m), were measured by carrying out differential scanning calorimetry (DSC) using a Perkin Elmer Pyris Diamond DSC (Perkin Elmer Instrument). The amount of polymer (N=3 per sample type) used for the study ranged from 8 to 10 mg and the sample was encapsulated in standard aluminium pans. All tests were conducted under inert nitrogen. The samples were heated/cooled/heated at a heating/cooling rate of 20^{o}C min^{-1} between -57^{o}C and 100^{o}C.Thermal gravimetric analysis (TGA) was conducted using a Stanton Redcroft STA-780 Series Thermal Analyzer, to determine the degradation profile. Scans were

performed between 10 and 1200^{o}C and at a rate of 5^{o}C min^{-1} Measurements were made over three repeats using a sample mass of 4 mg.

2.6. *In vitro* degradation studies

Degradation behaviour of the fabricated 2D films was studied for a period of 1, 2 and 4 months at 37°C in phosphate buffered saline (PBS) and Dulbecco's Modified Eagles Medium (DMEM). PBS was chosen since it is one of the buffer systems that regulate the acid or base balance in the body. DMEM was the culture medium used for the cytocompatibility studies with HaCaT cells and the fabricated films.

2.6.1. Water uptake, weight loss, pH measurements and surface studies

The degradation kinetics of the fabricated 2D films was determined by measuring the % water uptake or absorption (% WA) and % weight loss (% WL). All samples were first weighed to obtain the dry weight $M_{o,\ dry}$ ($M_{o,\ dry}$, the initial weight of the sample), immersed in the respective media and kept under static conditions at 37^{o}C. At each prescheduled incubation time point the films were collected and analysed for water absorption (% WA) and weight loss (% WL) behaviour. For measuring the % WA, the immersed samples were removed at given time points, the surface gently wiped with a tissue paper and then weighed to obtain $M_{t\ wet}$ ($M_{t\ wet,}$ the weight of the samples after immersion in the medium). Similarly, for measuring the % WL, the samples were withdrawn from the medium, washed several times with deionised water and dried at 37^{o}C overnight and subsequently weighed dry, to obtain $M_{t\ dry}$ ($M_{t\ dry}$, the dry weight of the samples after immersion in the media followed by drying). Water absorption and weight loss were calculated using the following equations:

$$\% \text{ WA} = [(M_t \text{ wet} - M_t \text{ dry})/M_t \text{ dry}]100$$

$$\% \text{ WL} = [(M_o \text{ dry} - M_t \text{ dry})/M_o \text{ dry}]\ 100$$

The media in which the films were incubated were changed every week for the first one month and every 14-16 days progressively. The pH of this incubated media was recorded. Surface degradation via SEM of the *in vitro* degraded films was carried out as described above.

2.7. Protein adsorption studies

Protein adsorption assay was performed using foetal bovine serum (FBS). Square films, (1 cm^2 in area), were incubated in 400 μL of undiluted FBS, at 37°C, for 24 hrs. After incubation, the samples were rinsed with PBS, three times. The samples were then incubated in 1 mL of 2% sodium dodecyl sulphate (SDS) in PBS for 24 hrs at room temperature and under vigorous shaking to further collect the adsorbed proteins. The amount of total protein adsorbed on the surface of the samples was quantified using a commercial protein quantification kit (Pierce, Rockford, IL). The optical density of the samples was measured spectrophotometrically at 562 nm against a calibration curve using bovine serum albumin as per the manufacturer's protocol. The samples incubated in PBS were used as a negative control. The assay was carried out in triplicates.

2.8. *In vitro* cytocompatibility study

The *in vitro* cell culture studies were carried out on the fabricated films (N=3 per sample type) using the Human keratinocyte cell line (HaCaT), which was cultured in DMEM growth medium, supplemented with 10% foetal calf serum, 1% glutamine and 1% penicillin and streptomycin solution. The cells were incubated at 37°C in a 5% CO_2 humidified atmosphere with the culture medium being changed every 2 days. The fabricated 2D films, 1 cm^2 in area, were UV sterilised for 30 minutes on each side and exposed in culture medium for 12 h in order to passivate the surfaces. 20,000 cells were seeded per cm^2 of the films, kept in 24 well plates. The cells were analysed after 1, 4 and 7 days for cell adhesion, proliferation and morphology. Cell adhesion and proliferation studies were carried out using the Neutral Red

(NR) assay as described elsewhere.[47] The total NR uptake was a measure of the cell proliferation and viability (% NR uptake is directly proportional to the number of live and uninjured cells and was compared to a control population grown on tissue culture plates. The control was normalised to 100%. The samples for SEM analysis of cell morphology were prepared as described in Misra *et al*.[25]

2.9. *In vitro* haemostatic study using Thromboelastograph®, TEG®

The haemostatic effect of the n-BG 45S5® was studied by thromboelastography using a TEG® 5000 series Hemostasis Analyzer (Medicell Ltd, London, UK). Briefly, 20 μl of 0.2M $CaCl_2$ was added to 360 μl of citrated whole blood, followed by controlled amounts of n-BG. The following clotting parameters were then monitored i.e. the R time (reflecting the time delay before the clotting process begins to be detectable), alpha angle (reflecting the rate at which clotting proceeds) and maximum amplitude (reflecting the strength of the formed clot). Three different amounts of n-BG 45S5® i.e. 1, 2 and 4 mg were used for the study, in order to look for dose-related changes.

2.10. Statistical analysis

The data sets have been expressed along with their mean standard deviation. The data, where appropriate, were compared using the student's t-test and differences were considered significant when $*p < 0.05$.

3. Results and discussion

The fabrications of the matrices, P(3HO) neat (control) and P(3HO)/n-BG composite films was successfully carried out using the solvent casting method. The surface morphology assessment by SEM revealed that the P(3HO) control films (**Figure 1(a-b)**) possessed a

smooth surface. However, in the case of P(3HO)/n-BG composite films, the incorporation of the n-BG changed the surface morphology by introducing nanotopographical features (**Figures 1(c-d))**. n-BG particles were found embedded in the matrix and deposited on the surface of the composite.

Figure 1

This incorporation of artificial nanotopography onto the surface of the P(3HO)/n-BG composite films resulted in enhanced roughness, as confirmed by surface scans, using white light interferometry (Zygo®). A typical root-mean-square-average (RMS) roughness value of 0.440 μm was determined for the 5wt% composite film as opposed to 0.238 μm for the 5 wt% neat (control) film. Roughness measurements of the 10 wt% films were not assessed; however similar observation of increased roughness of the 10 wt% composite could be expected. Static contact angle (θH_2O) measurements for the control and composite films were as follows: 5 wt % neat, θH_2O = 77°; 5 wt % composite = 75°, 10 wt% neat = 78 ° and 10 wt % composite = 76°. For the composite films, incorporation of n-BG resulted in increased wettability as revealed by the decreased static contact angle (n=4, *$p<0.05$).

To engineer a successful skin tissue for wound healing, the skin graft must provide epidermal coverage followed by subsequent restoration of the dermal layer. This is because epidermal coverage on its own fails to restore structural and functional integrity of the skin, thereby resulting in fragility of the graft, wound contraction and scar formation. In order to achieve this restoration of the dermis layer, a suitable matrix/scaffold to provide flexible and stable support to the epidermal coverage and nutrients to the keratinocytes in the epidermal layer is required.[4, 8] This stability of the keratinocyte attachment onto the wound bed becomes more challenging if the location of such wound beds is in difficult contours of the body. In such cases having a flexible and elastomeric support is essential. Therefore, in this context the

observation of increased Young's modulus and strength of the P3(HO)/n-BG nanocomposites due to the incorporation of the n-BG, with a concomitant maintenance of the elastomeric and flexible properties is an ideal, highly desirable outcome. The stress-strain curves of the fabricated films resembled that of elastomeric materials. (Stress strain profiles are provided as supplementary information, Figure S.1). The Young's modulus value calculated from the curves were: 5 wt% composite film = 3 ± 1 MPa, 5 wt% neat(control) film = 1.4 ± 0.6 MPa, 10 wt% composite film = 4 ±1 MPa and 10 wt% neat (control) film = 3.1 ± 0.7 MPa. Under the experimental conditions of this study, only the 5 wt% composite and 5 wt% neat films failed during the test; the tensile strength for the 5 wt% composite film was 3.3 MPa and that of the 5 wt % neat (control) film was 1.8 MPa. The % elongation of these films was: 5 wt% composite film = 236 % ± 10 and 5 wt% neat (control) film = 278 % ± 10. The % elongation at the end of the test for the other films were, 10 wt% composite film = 222 % ± 6 and 10 wt% neat (control) film = 257 % ± 9.

The increased Young's modulus and tensile strength of the composites owing to n-BG incorporation was similar to that observed for P(3HB)/n-BG composites [25], nanoscale tricalcium phosphate/PLGA composites [33] and poly(glycerol sebacate)/ Bioglass® 45S5 composites.[34] This effect can be explained first by the efficient infiltration and sealing of the pores in the polymer matrix by the n-BG, thereby strengthening the whole composite structure. Secondly, the incorporation of the n-BG into the polymer matrix provides a higher interfacial surface area which enhances the load transfer between the polymer matrix and the stiff n-BG inclusions. The P(3HO)/n-BG composite developed also showed reduction in their melting temperature (Table 1), thus corresponding to a decrease in their crystallinity when compared to P(3HO) control films. This decrease in crystallinity possibly occurred due to the incorporation of n-BG particles in the crystalline portion of the polymer matrix which resulted in disruption and reduction of the ordered arrangement of the P(3HO) polymeric chains in the

composite. A similar observation of decrease in the T_m was also reported when n-BG was incorporated into the P(3HB) matrix. The melting temperature reduced from 172°C for P(3HB) neat film to 156°C, 157°C and 155°C for P(3HB) containing 10, 20 and 30 wt% of n-BG, respectively.[25]

Table 1

Thermogravimetry analysis (provided as supplementary information, Figure S.2) revealed that the P(3HO) control films lost all its weight at 300°C, similar to that of P(3HB-co-3HHx).[35] Incorporation of n-BG reduced the degradation temperature to 195°C for the 5 wt% composite and to 200°C for the 10 wt% composite film. This initial reduction in mass could be due to the loss of water which was incorporated in the 45S5 Bioglass® mass, as described by Clupper and Hench.[36] Also for the composites (Figure S-2) the weight loss was rapid up to 250°C but remained constant after about 500°C, implying that at this point the entire polymer was burnt off and only n-BG was left.

When investigated for *in vitro* degradation behaviour, the developed samples underwent surface degradation via abiotic non enzymatic hydrolysis occurring due to the cleavage of the ester bond in the P(3HO) backbone, typical of the PHA family. The % of water absorbed (WA) and weight loss (WL) by the films are depicted in **Figure 2(a-d)** respectively. Since, hydrolytic degradation of PHAs is known to be a slow process when compared to the enzymatic hydrolysis of PHAs [37], this explains why only a maximum weight loss of 18 % was observed for the P(3HO)/n-BG system as opposed to the control film which was 15 %. This low degradation is also due to the hydrophobic nature of the long alkyl pendant chains of the P(3HO) polymer.[38] The increased water absorption and weight loss demonstrated by the composites was due to its decreased crystallinity and the hydrophilic nature of the n-BG

particles. Similar results of increased water absorption and weight loss were observed for P(3HB)/n-BG composites.[25, 32] Surface studies of the degrading films using SEM **(Figure 2(g-h))**, at the end of 4 months of incubation, showed degraded polymer surface with loose polymer flakes present on the surface, suggesting that the films underwent surface degradation. This surface degradation behaviour of the developed composites is also advantageous as opposed to polymeric matrices e.g. poly(glycolic acid-co-lactic acid) (PLGA) which undergo bulk degradation. In a skin tissue engineering situation, where the stability of the matrix/support is also crucial for delivering the keratinocyte epidermal layer in to the wound site, use of a bulk degrading matrix may be unfavourable and would lead to wound contraction due to premature loss of geometry of the matrix. On the other hand such wound contraction will be avoided using the developed P(3HO)/n-BG composite, which is able to maintain its geometry during degradation. Also, as the PHA family is bioresorbable, hence P(3HO)/n-BG matrix would be resorbed in the body, thus avoiding surgical intervention needed to remove the matrix support.

Figure 2

45S5 Bioglass® has been shown to have an antibacterial effect against *S.aureus* and *S. epidermis* which are bacterial strains found quite often in wound dressing. Pratten *et al*.[39] found that bacterial colonization decreased significantly on surgical sutures with bioactive glass coating, as compared to those without coating. This bactericidal effect of Bioglass® 45S5 has been attributed to high pH caused by the dissolution of the alkali ions from the glass and an additional ion release.[40] In this present study, leaching of alkaline and calcium ions from the P(3HO)/n-BG system resulted in an increase of pH in both DMEM and PBS medium **(Figure 2 (e-f))**. The increase in pH of the P(3HO) control films occurred because all the 3HO molecules existed in the base form, i.e. 3-hydroxyoctanoate.[20] The pH of the media at the end of 4 months of incubation was around 9.2-9.4 in DMEM and 7.8 in PBS media. In addition,

the ion release products of Bioglass® particles have also been known to possess angiogenic potential. Achieving vascularizaton is crucial for the success of a functional tissue engineered construct. The ion release products from the Bioglass® have been shown to up regulate the expression of angiogenic factors such as vascular endothelial growth factor (VEGF).[29, 30] In this respect the developed nanocomposite has yet another added advantage, as the ion release products from the nanocomposite films can also aid in the vascularisation of the engineered skin tissue construct.

The bioactive glass nanoparticles used in this investigation were also found to be haemostatically active. As reported by Ostomel *et al*. for mesoporous bioglass particles the haemostatic activity of the 45S5 Bioglass® particles could also be due to its dual role of supplying calcium ions, which act as cofactors for initiating the blood clotting cascade, and also by providing a negatively charged siliceous oxide as a support for surface dependent thrombotic reactions. The bioglass particles accelerated the time for blood clot formation, however, the clot formed was of reduced strength as opposed to the control (whole human blood only) (Table 2). This observation could be due to the low Si to Ca ratio for the n-BG which is 1.69. Ostomel *et al*. in their work demonstrated that the clotting time and the clot strength was affected by the composition of the bioglass; mesoporous bioglass particles with a high silicon (Si) to calcium (Ca) ratio of 80, was more haemostatic than that of Si to Ca ratio of 60.[31] From these studies it can therefore be hypothesized that the tissue engineered skin graft developed using these P(3HO)/n-BG nanocomposite matrices when grafted onto the wound site will provide healthy cells as well as prevent blood loss following tissue injury, due to the haemostatic effect of the bioactive glass nanoparticles, a great advantage.

Table 2

Mammalian cells are anchorage dependent and need a biocompatible, protein rich surface for attachment, differentiation and migration to form new tissue.[25, 41, 42] Therefore, protein adsorption assay was carried out to indirectly evaluate cell adhesion and survival on the fabricated films. In this study, analysis was carried out using the whole protein serum. The amount of protein adsorbed on the films were: 5 wt% composite film = 140 μg/cm^2, 5 wt% neat (control) film = 75 μg/cm^2, 10 wt% composite film = 130 μg/cm^2 and 10 wt % neat (control) film = 83 μg/cm^2. The protein adsorption was significantly higher (n=4, **p<0.01) on the P(3HO)/n-BG composite films than on the P(3HO) neat (control) films. Surface properties of a material, both chemical composition and topographical features play an important role in the adsorption behaviour of proteins. Therefore, this increased adsorption of proteins on the composite films could be due to the incorporation of the n-BG which had increased the surface roughness, hydrophilicity and also the surface area of the composite exposed to proteins. This result is in agreement with the increased adsorption of proteins observed on composites of P(3HB)/n-BG,[25] nanoscale hydroxyapatite/PLLA composite film [41] and fibrous nanoscale tricalcium phosphate/PLGA composite scaffolds.[43] This increased adsorption of proteins on the P(3HO)/n-BG composite system also translated into improved biocompatibility of the composite as opposed to the control for the seeded HaCaT cells. The growth of HaCaT cells increased progressively with time, also better attachment and proliferation of cells on composite films was observed, as opposed to the P(3HO) control films. At day 7 there was a significant increase in the growth of cells on composite films when compared to neat (control) films and the control (n = 4, **p<0.05). Keratinocytes are known to form four distinct layers that divide and differentiate as they move from the deeper layer to the outermost layers. This arrangement of cell layers from the bottom to the outermost is as follows: (1) stratum basale (basal layer), (2) stratum spinulosum (spiny or prickle cell layer), (3) stratum granulosum (granular layer) and (4) stratum corneum (horn

sheet layer).[44] The morphology, attachment and proliferation of the seeded HaCaT cells on the fabricated films, as revealed via SEM, is shown in **Figure 3(a-b)**. In the neat control films confluent growth was observed by day 4, **Figure 3(c-d)**, however, horn sheets were only observed by day 7. Coherent horn sheets of the stratum corneum were observed by day 4 in both the 5 and 10 wt% composite films. As horn sheets are the outermost and most mature or differentiated stage of the HaCaT cell line, this implies that the cells had successfully attached, proliferated and grown on the fabricated composite films, **Figure 3(e-f)**.

Figure 3

These SEM observations confirm that the HaCaT cells were able to proliferate better on the composite films as opposed to the neat (control) films. It has been discussed in literature that a rough and hydrophilic surface provides a better matrix for cell attachment and proliferation.[35, 45] Hence, the incorporation of the rough nanotopography, increased wettability and high surface area of the P(3HO)/n-BG composite system enabled improved adhesion, growth and proliferation of the HaCaT cells on the composite as opposed to the P(3HO) control. Similar observation of increased MG-63 osteoblast proliferation was observed for P(3HB)/n-BG composites, in comparison to the neat P(3HB) scaffolds, by Misra *et al*.[25] and increased proliferation of MC3T3-E1 osteoprogenitor cells on P(3HB-co-3HHx)/ hydroxyapatite scaffolds, when compared to P(3HB-co-3HHx) scaffold.[35] A schematic representation of the developed P(3HO)/n-BG nanocomposite as matrix support for engineering skin tissue is shown in Figure 4.

Figure 4

4. Conclusions

In summary we have developed a novel P(3HO)/n-BG nanocomposite system with numerous unique features including highly elastomeric nature, high surface topography and hydrophilicity, haemostatic properties, ability to enhance vascularization, antibacterial activity and high biocompatibility. The composite is amenable to thermal processing, revealed surface degradation properties, ideal for maintaining matrix integrity whilst undergoing degradation and exhibited the required elastomeric mechanical properties. Considering all these features in the newly developed P(3HO)/n-BG nanocomposite system, we conclude that this work has led to the development of a unique matrix with an extraordinary potential for engineering skin tissue.

Acknowledgements

The authors would like to thank the Quentin Hogg Foundation and the School of Life Sciences of the University of Westminster for the financial support to carry out this study. This work was supported in part (JCK) by WCU Program through the National Research Foundation of Korea (NRF) funded by the Ministry of Education, Science and Technology (No. R31-10069).

Running head: P(3HO)/n-BG composite for TE application

References

[1] MacNeil, S. *Nature* **2007**, 445, 874.
[2] Groeber, F.; Holeiter, M.; Hampel, M.; Hinderer, S.; Schenke-Layland, K. *Adv. Drug. Deliv. Rev*. **2011**, 128, 352.
[3] Falanga, V.; Faria, K.; Lanza, R.; Vacanti, J. P. Bioengineered skin constructs. In: Principles of Tissue Engineering, Lanza, R., Langer, R., and Vacanti, J. P., editors. Academic Press, Burlington, VT, 2007; pp. 1167–1185.
[4] Zhong, S. P.; Zhang, Y. Z.; Lim, C. T. *WIREs Nanomed. Nanobiotechnol*. **2010**, 2, 510.
[5] Tsuruta, D.; Green, K. J.; Getsios, S.; Jones, J. C. R. *Trends Cell Biol*. **2002**, 12, 355.
[6] Kaustabh, G.; Clark, R. A. F.; Lanza, R.; Langer, R.; Vacanti, J. Wound repair. In: Principles of Tissue Engineering, Lanza, R., Langer, R., and Vacanti, J. P., editors. Academic Press, Burlington, VT, 2007; pp. 1149–1166.
[7] Allgower, M.; Schoenberger, G. A.; Sparkes, B. G. *Burns* **1995**, 21, S7.
[8] Nair, L. S.; Laurencin, C. T. *Adv. Biochem. Eng. Biotechnol*. **2006**, 102, 47.
[9] Mason, C. *Med. Dev. Technol*. **2005**, 16, 32.
[10] Katti, D. S.; Laurencin, C. T. Synthetic biomedical polymers for tissue engineering and drug delivery. In: Advanced polymeric materials: structure and property relationship, Shonaike, G., and Advani, S. G., editors. CRC Press, Washington, DC, 2003; pp. 479–525.
[11] Li, W. J.; Laurencin, C. T.; Caterson, E. J.; Tuan, R. S.; Ko, F. K. *J. Biomed. Mater. Res A* **2002**, 60, 613.
[12] Dhandayuthapani, B.; Krishnan, U. M.; Sethuraman, S. *J. Biomed. Mater. Res. B* **2001**, 94, 264.
[13] Kuppan, P.; Vasanthan, K. S.; Sundaramurthi, D.; Krishnan, U. M.; Sethuraman, S. *Biomacromolecules* **2011**, 12, 3156.
[14] Terskiih, V. V.; Vasiliev, A. V. *Int. Rev. Cytol*. **1999**, 188, 41.
[15] Peschel, G.; Dahse, H. M.; Konrad, A.; Wieland, G. H.; Mueller, P. J.; Martin, D. P.; Roth, M. *J. Biomed. Mater. Res*. **2008**, 85, 1073.
[16] Lütke-Eversloh, T.; Fischer, A.; Remminghorst, U.; Kawada, J.; Marchessault, R. H.; Bögershausen, A.; Kalwei, M.; Eckert, H.; Reichelt, R.; Liu, S. L.; Steinbüchel, A. *Nat. Mater*. **2002**, 1, 236.
[17] Rehm, B. H. A. *Nat. Rev. Microbiol*. **2010**, 8, 578.
[18] Rai, R.; Keshavarz, T.; Roether, J. A.; Boccaccini, A. R.; Roy, I. *Mater. Sci. Eng. R* **2010**, 72, 29.
[19] Rai, R.; Darmawati, M. Y.; Boccaccini, A. R.; Knowles, J. C.; Barker, I.; Howdle, S. M.; Tredwell, G. D.; Keshavarz, T.; Roy, I. *Biomacromolecules* **2011**, 12, 2126.
[20] Rai, R.; Boccaccini, A. R.; Knowles, J. C.; Mordon, N.; Salih, V.; Locke, I.; Torbati, M. M.; Keshavarz, T.; Roy, I. *J Appl. Polym. Sci*. **2011**, 122, 3606.
[21] Misra, S. K.; Valappil, S. P.; Roy, I.; Boccaccini, A. R. *Biomacromolecules* **2006**, 7, 2249.
[22] Rezwan, K.; Chen, Q. Z.; Blaker, J. J.; Boccaccini, A. R. *Biomaterials* **2006**, 27, 3413.
[23] Hench, L. L. *J. Am. Ceram. Soc*. **1998**, 81, 1705.
[24] Chen, Q. Z.; Roether, J. A.; Boccaccini, A. R. Tissue engineering scaffolds from bioactive glass and composite materials. In: Topics in tissue engineering, vol. 4, Ashammakhi, N., Reis, R., and Chiellini, F., editors. 2008; Chap. 6.
[25] Misra, S. K.; Mohn, D.; Brunner, T. J.; Stark, W. J.; Philip, S. E.; Roy, I.; Salih, V.; Knowles, J. C.; Boccaccini, A. R. *Biomaterials* **2008**, 29, 635 1750.
[26] Mohn, D.; Bruhin, C.; Luechinger, N. A.; Stark, W. J.; Imfeld, T.; Zehnder, M. *Int. Endo. J*. **2010**, 43, 1037.
[27] Waltimo, T.; Brunner, T. J.; Vollenweider, M.; Stark, W. J.; Zehnder, M. J. *Dent. Res*. **2007**, 86, 754.

[28] Edwards, R.; Harding, K. *Curr. Opin. Infect. Dis*. **2004**, 17, 91.
[29] Day, R. M. *Tissue Eng*. **2005**, 11, 768.
[30] Leu, A.; Stieger, S. M.; Dayton, P.; Ferrara, K. W.; Leach, J. K. *Tissue. Eng. Part A* **2009**, 15, 877.
[31] Ostomel, T. A.; Shi, Q.; Tsung, C. K.; Liang, H.; Stucky, G. D. *Small* **2006**, 2, 1261.
[32] Misra, S. K.; Nazhat, S. N.; Valappil, S. P.; Torbati, M. M.; Wood, R. J. K.; Roy, I.; Boccaccini, A. R. *Biomacromolecules* **2007**, 8, 2112.
[33] Loher, S.; Reboul, V.; Brunner, T. J.; Simonet, M.; Dora, C.; Neuenschwander, P. *Nanotechnology* **2006**, 17, 2054.
[34] Liang, S. L.; Cook, W. D.; Thouas, G. A.; Chen, Q.Z. *Biomaterials* **2010**, 31, 8516.
[35] Xi, J.; Zhang, L.; Zheng, Z.; Chen, G.; Gong, Y.; Zhao, N.; Zhang, X. *J. Appl. Biomater. Appl*. **2008**, 22, 293.
[36] Clupper, D. C.; Hench, L. L. J. Non-Cryst. *Solids* **2003**, 43, 318.
[37] Marois, Y.; Zhang, Z.; Vert, M.; Deng, X.; Lenz, R.; Guidone, R. *J. Biomed. Mater. Res.* **2000**, 49, 216.
[38] Renard, E.; Walls, W.; Guerin, P.; Langlois, V. *Polym. Degrad. Stabil*. **2004**, 85, 779.
[39] Pratten, J.; Nazhat, S. N.; Blaker, J. J.; Boccaccini, A. R. *J. Biomater. Appl*. **2004**, 9, 47.
[40] Gubler, M.; Brunner, T. J.; Zehnder, M.; Waltimo, T.; Sener, B.; Start, W. J. *Int. Endo. J.* **2008**, 41, 670.
[41] Wei, G.; Ma, P. X. *Biomaterials* **2004**, 25, 4749.
[42] Webster, T. J.; Ergun, C.; Doremus, R. H.; Siegel, R. W.; Bizios, R. *J. Biomed. Mater. Res.* **2000**, 51, 475.
[43] Schneider, O. D.; Loher, S.; Brunner, T. J.; Uebersax, L.; Simonet, M.; Grass, R. N. *J. Biomed. Mater. Res. Part B* **2008**, 84B, 350.
[44] DermNet New Zealand. Structure of normal skin. 2010. http:// 670 dermnetnz.org/pathology/skin-structure.html
[45] Mei, N.; Zhou, P.; Pan, L. F.; Chen, G.; Wu, C. G.; Chen, X.; Shao, Z. Z.; Chen, G. Q. *J. Mater. Sci. Mater. Med.* **2006**, 17, 749.
[46] Brunner, T. J.; Grass, R. N.; Stark, W. J. Chem. Commun. 2006, 13, 1384.
[47] Prashar, A.; Locke, I. C.; Evans, C. S. *Cell Prolif*. **2004**, 37, 221.

Figure captions:

Figure 1: SEM images of the P(3HO) neat (control) and P(3HO)/n-BG nanocomposite films: (a) cross section and (b) planar surface of a 5 wt % P(3HO) neat (control) film revealed a smooth surface. (c) cross section and (d) planar surface of a 5 wt % (P(3HO)/n-BG) composite film revealed a rough surface. Arrows indicate the surface of the fabricated matrices; dashed circle with asterisk highlight the rough surface topography of the P(3HO)/n-BG due to the presence of the n-BG particles and its corresponding agglomeration.

Figure 2: *In vitro* degradation behaviour of the P(3HO)/n-BG and P(3HO) control samples showing the profiles for water absorption, weight loss and pH in DMEM medium (a, c, e)

and PBS medium (b, d, f). Surface degradation behaviour observed via SEM at the end of 4 months of incubation in DMEM medium of a 5 wt% composite film (g) and a 5 wt % neat control film (h).

Figure 3: SEM images of the seeded HaCaT cells on the fabricated films: (a-b) Seeded HaCaT cells showing attachment and proliferation on the film: (a) Magnification 2000X (b) Magnification 3000X; (c-d) Seeded HaCaT cells at day 4, on the neat film, confluent growth of the cells observed: (c) Magnification 2000X (d) Magnification 3000X; (e-f) Seeded HaCaT cells on day 7 on the composite film, arrangement of cells in horn sheets: (e) Magnification 2000X (f) Magnification 3000X: (1) Uncovered polymer matrix, (2) Cell layer and (3) Spreading of the cells.

Figure 4: Skin tissue regeneration based on a nanocomposite of P(3HO) and bioactive glass nanoparticles.

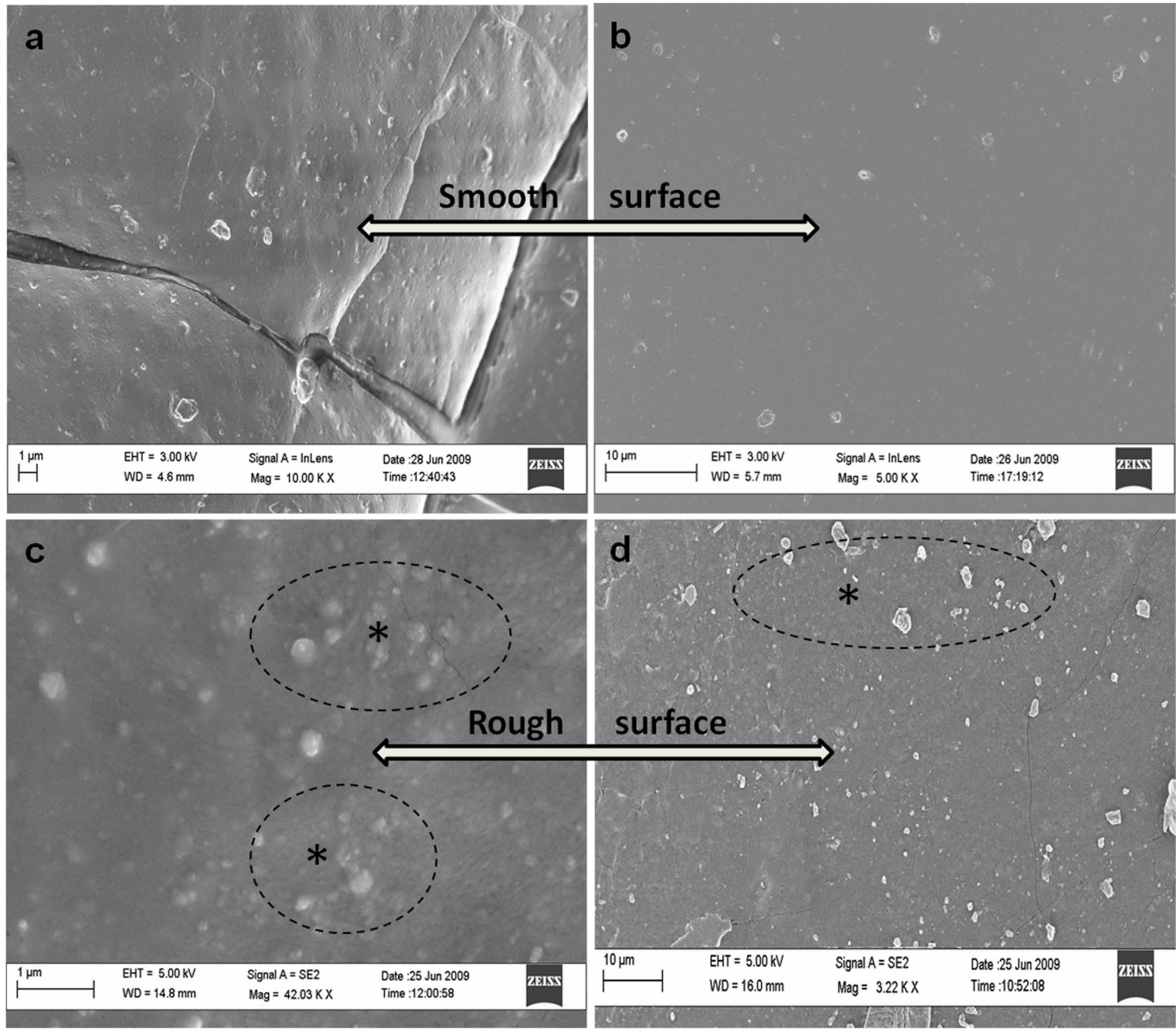
a
Smooth
surface
1 µm
EHT = 3.00 kV
WD = 4.6 mm
Signal A = InLens
Mag = 10.00 K X
Date :28 Jun 2009
Time :12:40:43
ZEISS
b
10 µm
EHT = 3.00 kV
WD = 5.7 mm
Signal A = InLens
Mag = 5.00 K X
Date :26 Jun 2009
Time :17:19:12
ZEISS
c
*
*
Rough
surface
1 µm
EHT = 5.00 kV
WD = 14.8 mm
Signal A = SE2
Mag = 42.03 K X
Date :25 Jun 2009
Time :12:00:58
ZEISS
d
*
10 µm
EHT = 5.00 kV
WD = 16.0 mm
Signal A = SE2
Mag = 3.22 K X
Date :25 Jun 2009
Time :10:52:08
ZEISS

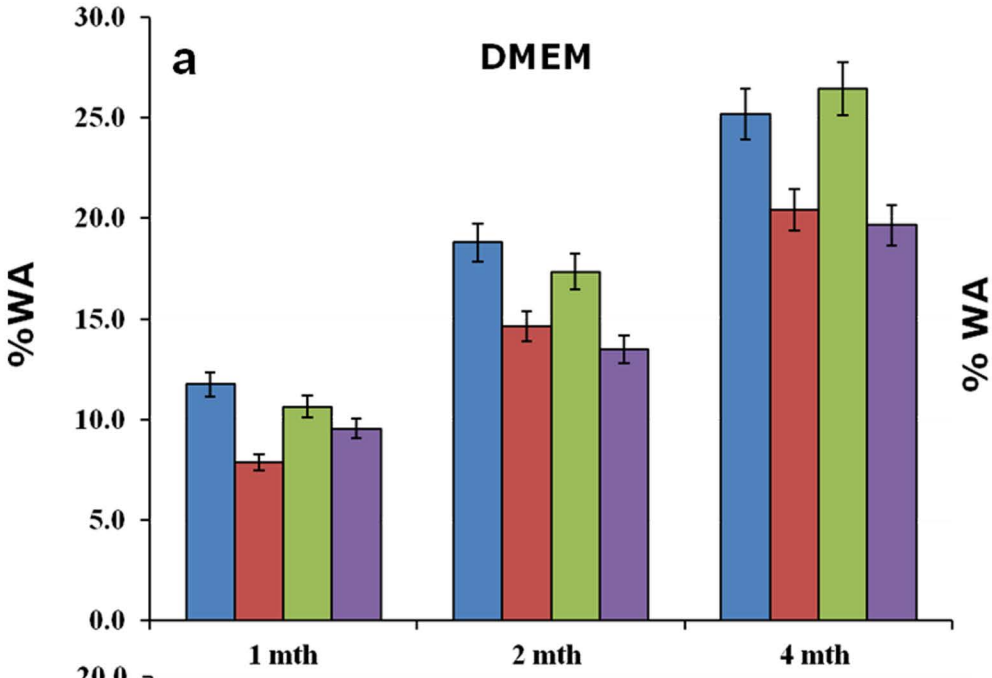
a
DMEM
%WA
30.0
25.0
20.0
15.0
10.0
5.0
0.0
1 mth
2 mth
4 mth

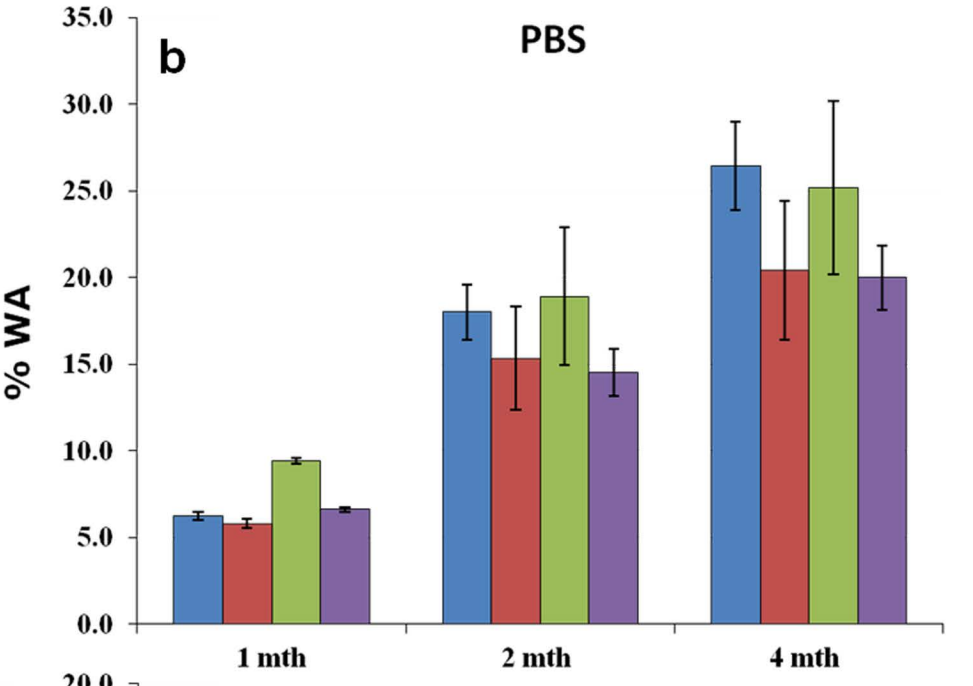
b
PBS
% WA
35.0
30.0
25.0
20.0
15.0
10.0
5.0
0.0
1 mth
2 mth
4 mth

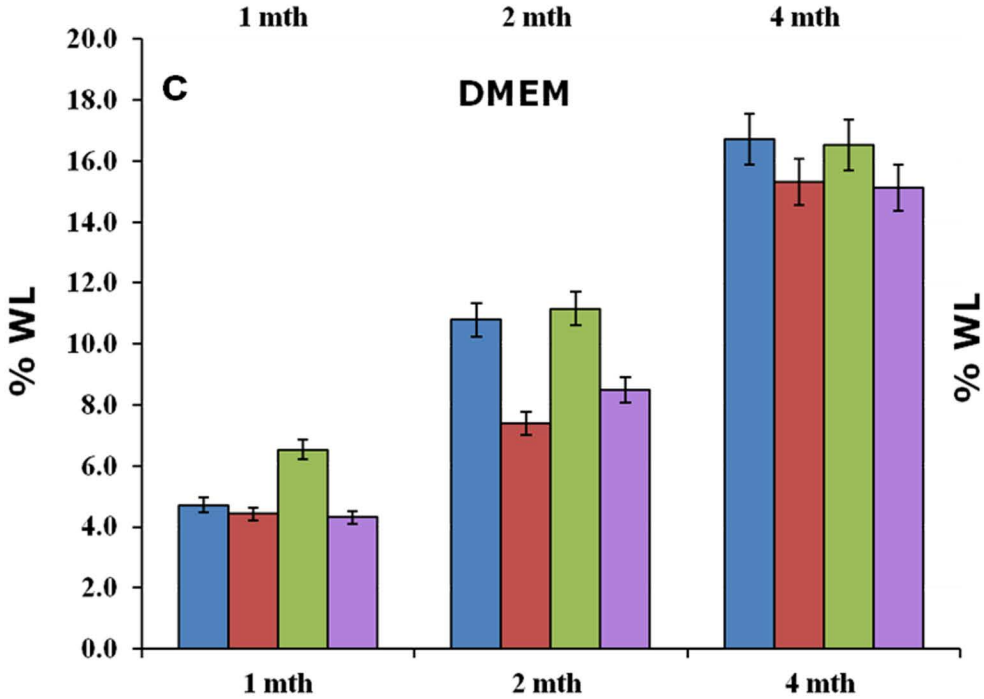
c
DMEM
% WL
20.0
18.0
16.0
14.0
12.0
10.0
8.0
6.0
4.0
2.0
0.0
1 mth
2 mth
4 mth

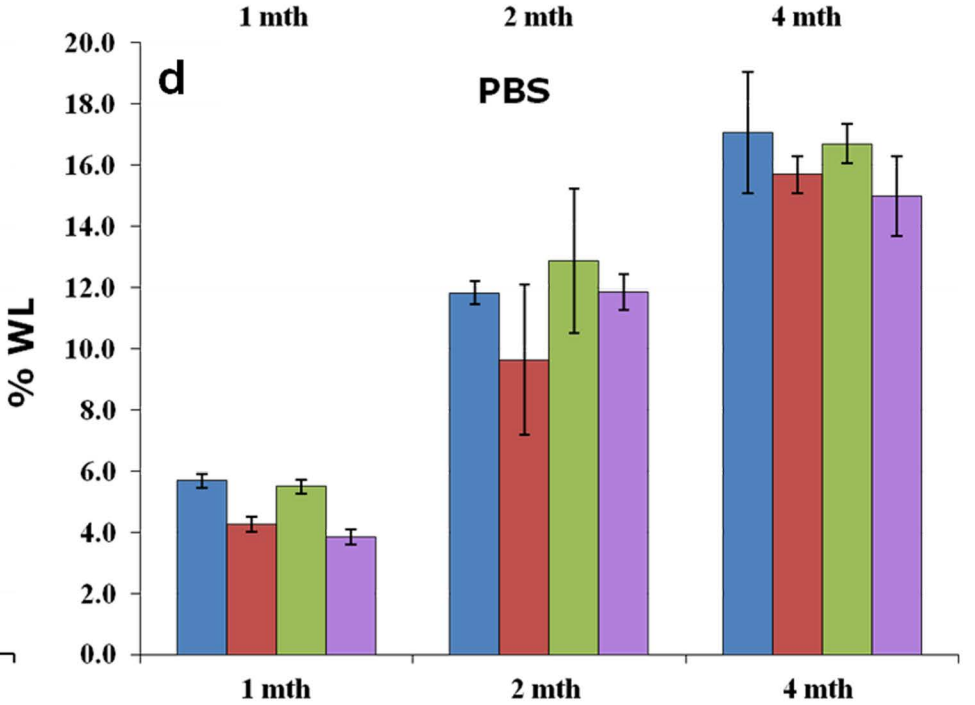
d
PBS
% WL
20.0
18.0
16.0
14.0
12.0
10.0
8.0
6.0
4.0
2.0
0.0
1 mth
2 mth
4 mth

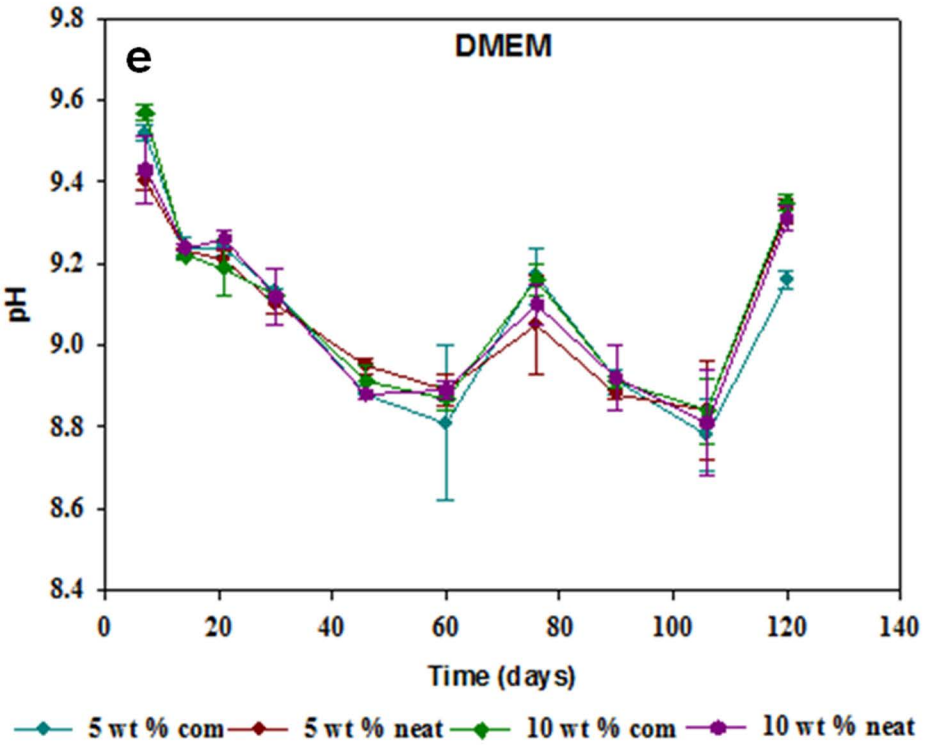
e
DMEM
pH
9.8
9.6
9.4
9.2
9.0
8.8
8.6
8.4
0
20
40
60
80
100
120
140
Time (days)
5 wt % com
5 wt % neat
10 wt % com
10 wt % neat

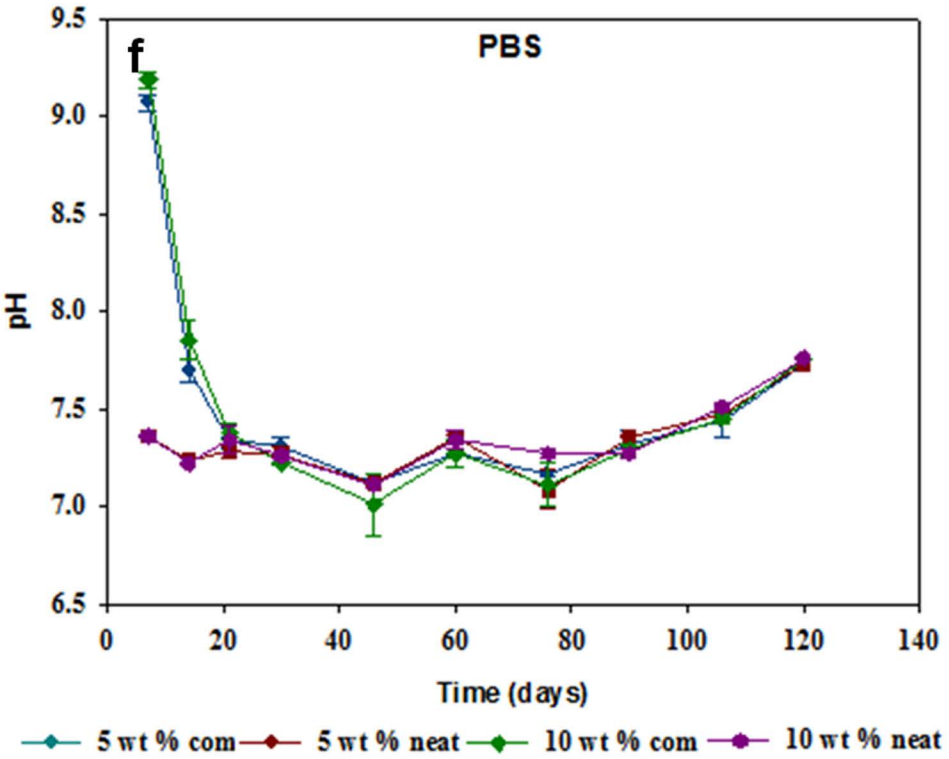
f
PBS
pH
9.5
9.0
8.5
8.0
7.5
7.0
6.5
0
20
40
60
80
100
120
140
Time (days)
5 wt % com
5 wt % neat
10 wt % com
10 wt % neat

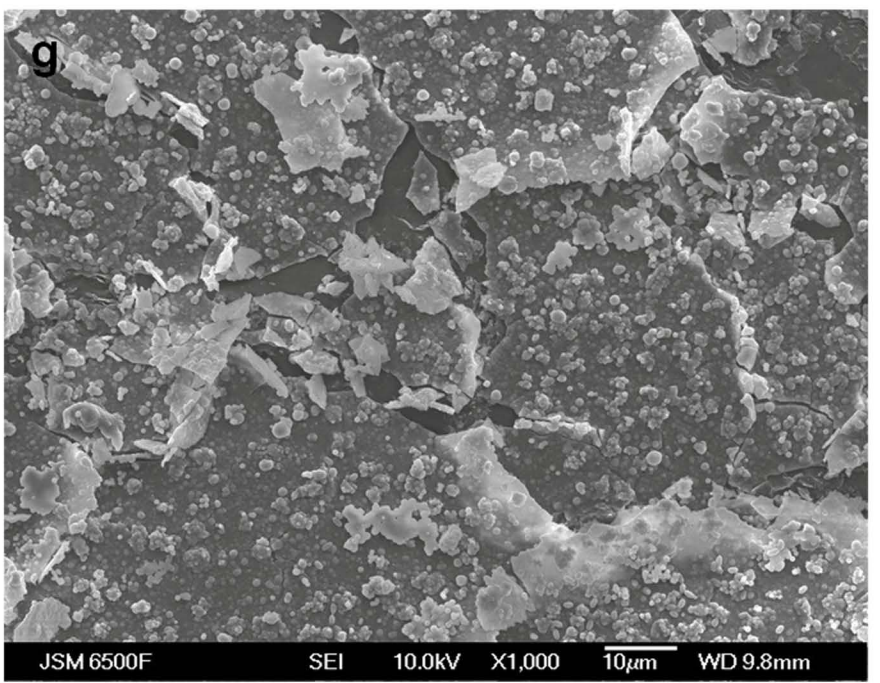
g
JSM 6500F
SEI
10.0kV
X1,000
10μm
WD 9.8mm

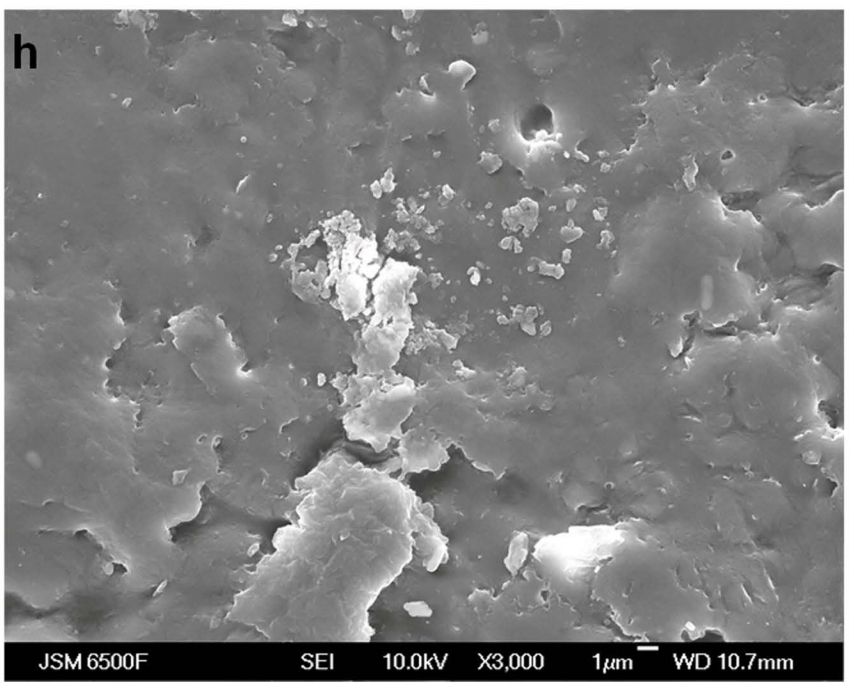
h
JSM 6500F
SEI
10.0kV
X3,000
1μm
WD 10.7mm

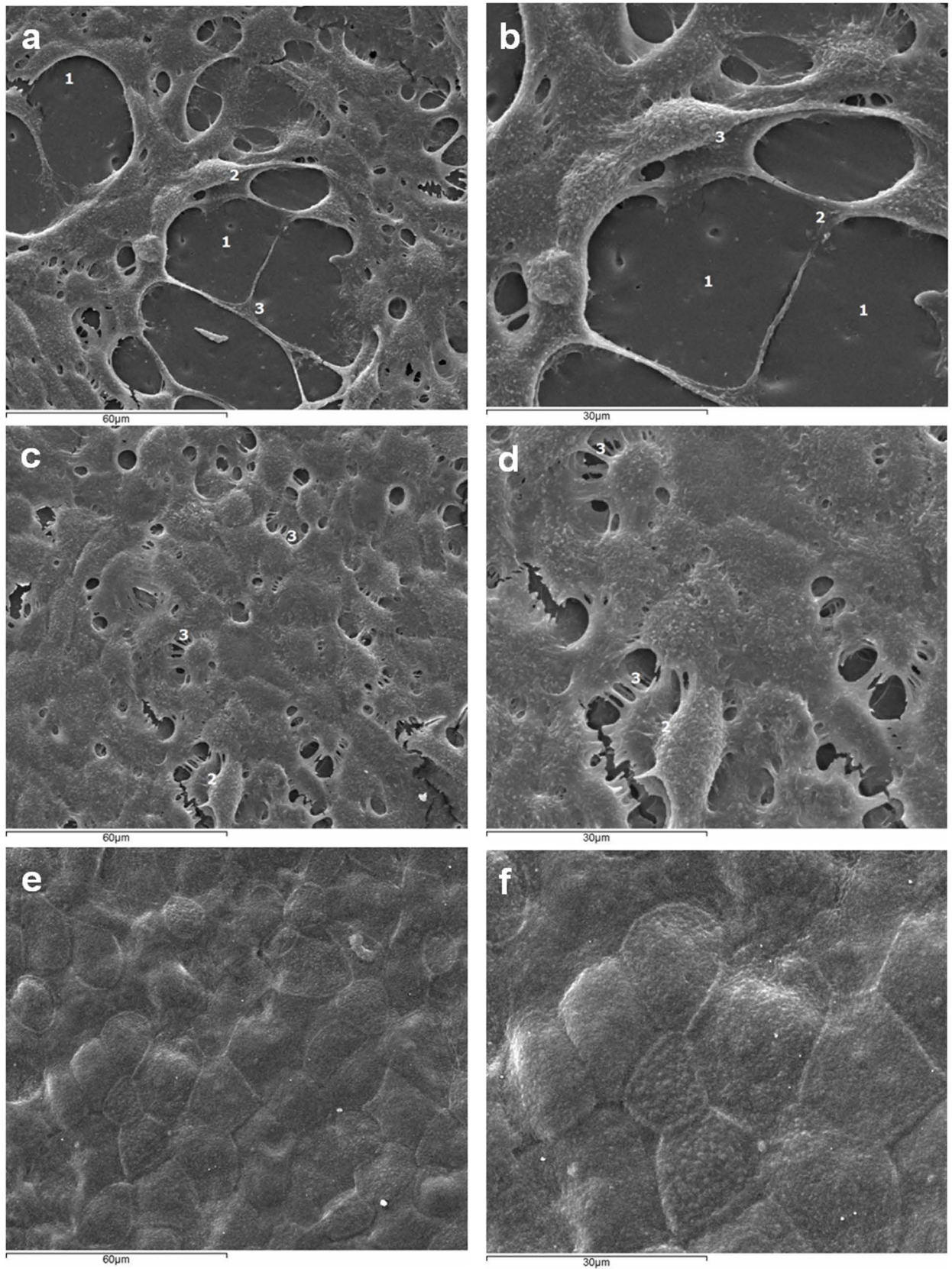
a
1
2
1
3
60µm
b
3
2
1
1
30µm
c
3
3
2
60µm
d
3
3
2
30µm
e
60µm
f
30µm

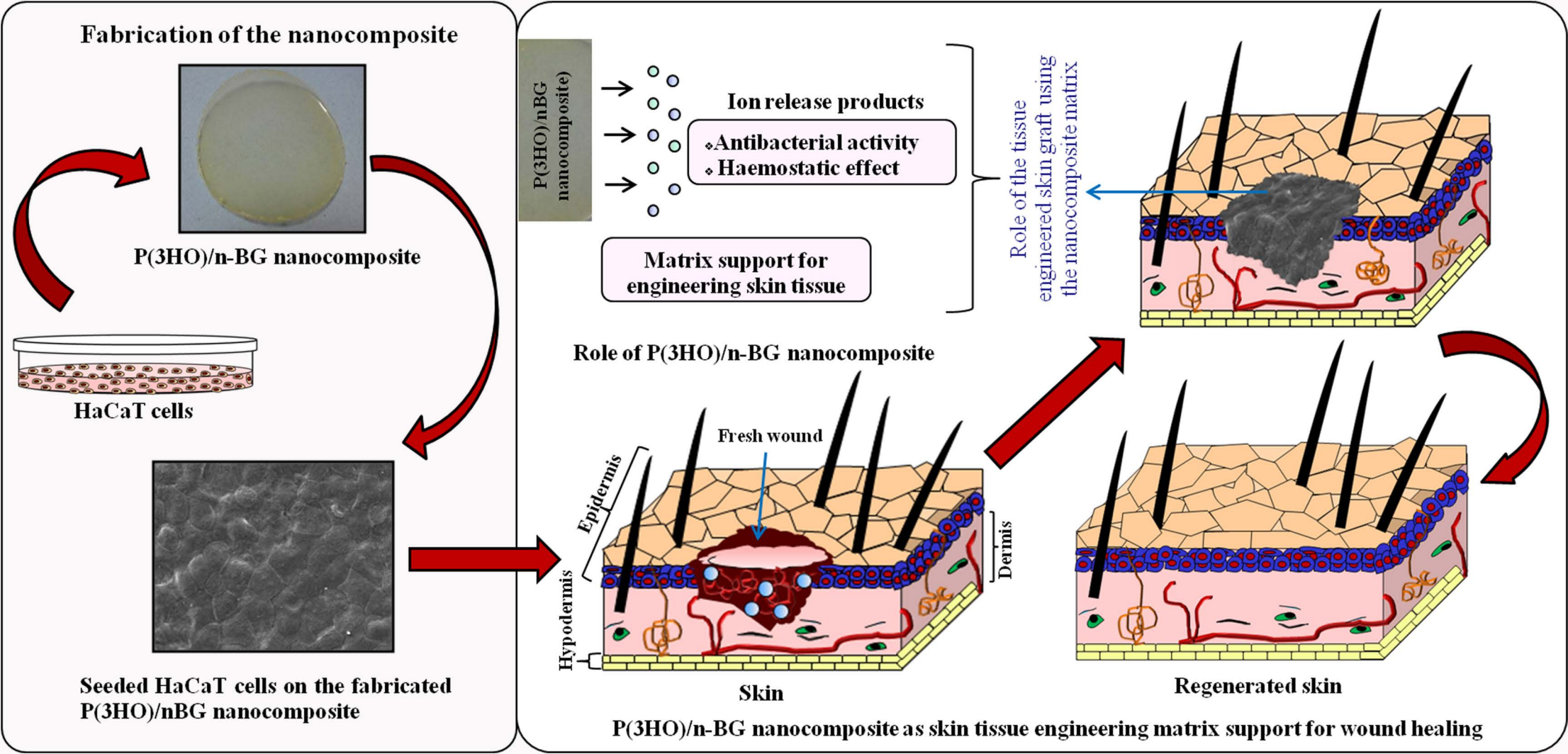
Fabrication of the nanocomposite
P(3HO)/n-BG nanocomposite
HaCaT cells
Seeded HaCaT cells on the fabricated P(3HO)/nBG nanocomposite
P(3HO)/nBG nanocomposite)
Ion release products
Antibacterial activity
Haemostatic effect
Matrix support for engineering skin tissue
Role of the tissue engineered skin graft using the nanocomposite matrix
Role of P(3HO)/n-BG nanocomposite
Fresh wound
Epidermis
Dermis
Hypodermis
Skin
Regenerated skin
P(3HO)/n-BG nanocomposite as skin tissue engineering matrix support for wound healing

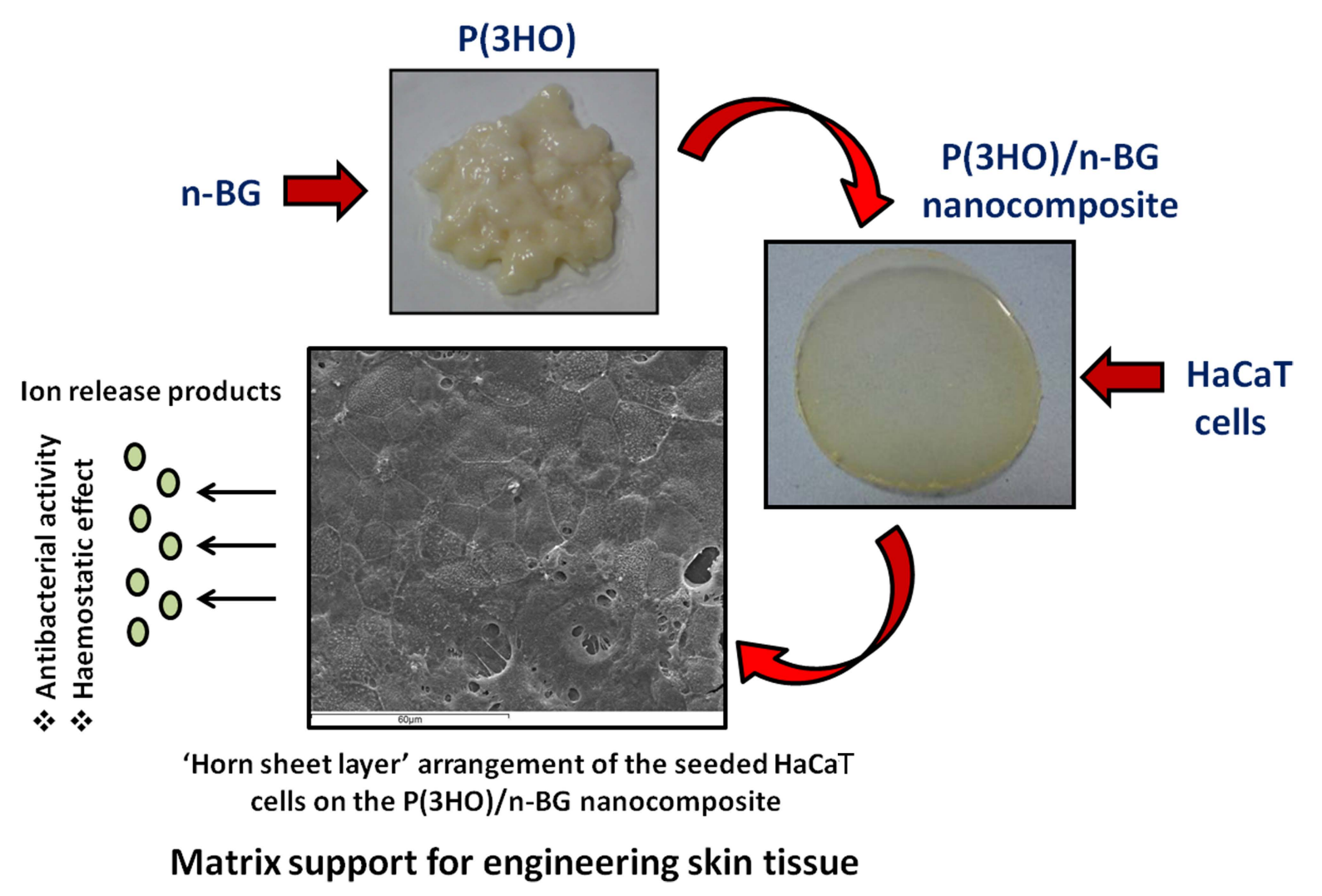

'Horn sheet layer' arrangement of the seeded HaCaT cells on the P(3HO)/n-BG nanocomposite

Matrix support for engineering skin tissue

Supporting information:

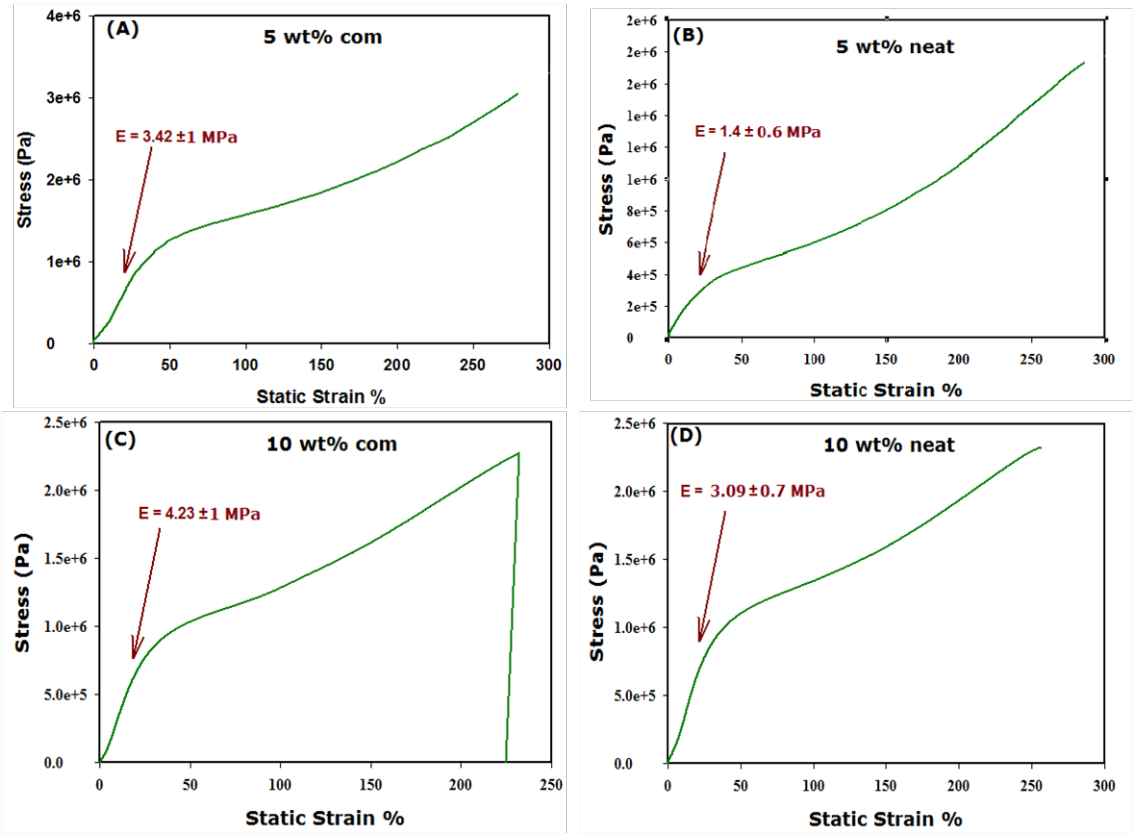

Figure S.1: Stress strain profile of the fabricated films: (A): 5 wt% composite film (B): 5 wt% neat film (control) (C): 10 wt% composite film (D): 10 wt% neat film (control). The films were subjected to a load between 200 to 6000 N which was increasing at the rate of 200N min^{-1}.

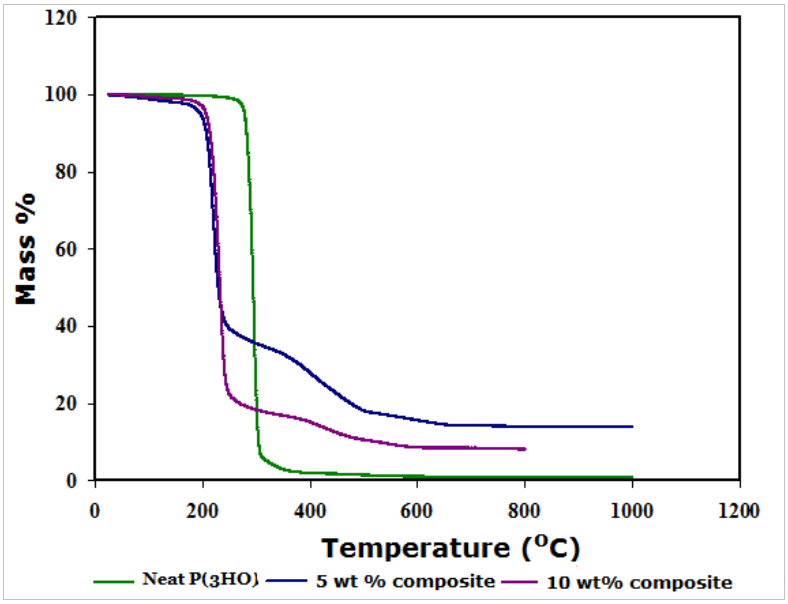

Figure S.2: Thermogravimetric profile of the fabricated films. Scan showing the changes in the mass of the (a) P(3HO) neat film (control) (b) 5 wt% composite film and (c) 10wt % composite film as a function of temperature.

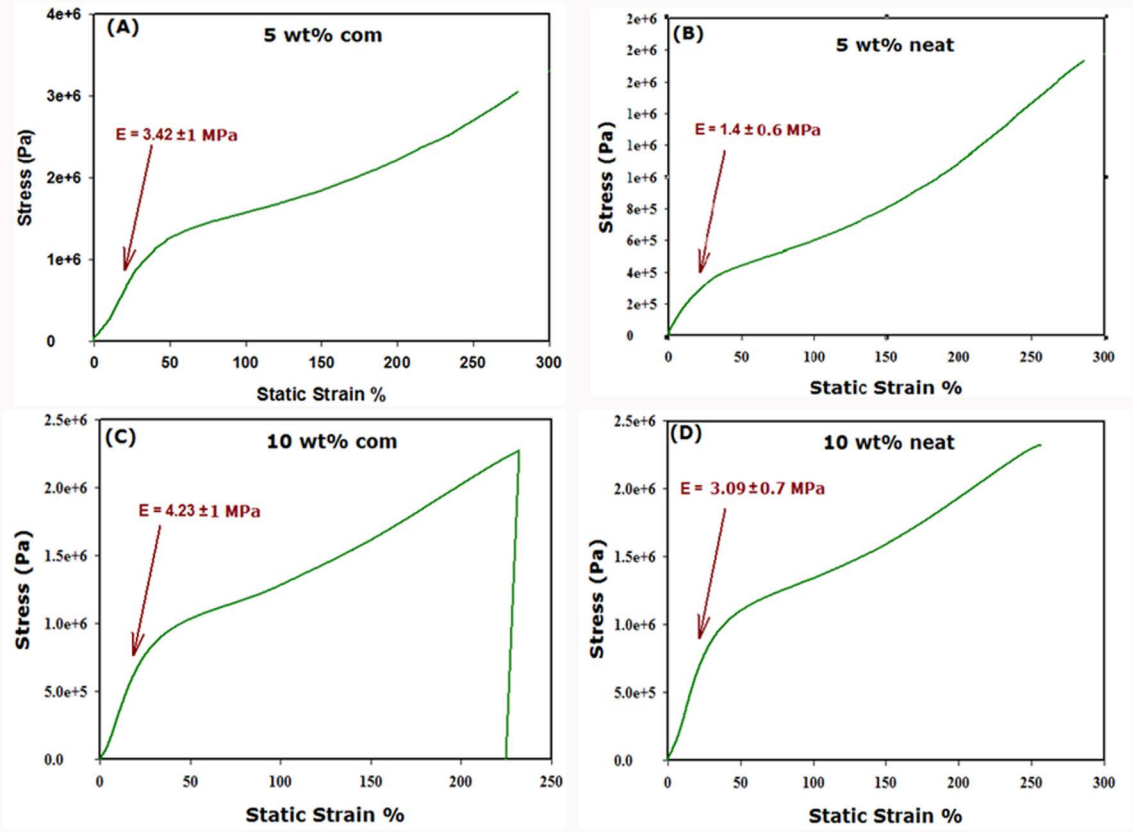
(A)
5 wt% com
E = 3.42 ±1 MPa
Stress (Pa)
Static Strain %
(B)
5 wt% neat
E = 1.4 ± 0.6 MPa
Stress (Pa)
Static Strain %
(C)
10 wt% com
E = 4.23 ±1 MPa
Stress (Pa)
Static Strain %
(D)
10 wt% neat
E = 3.09 ± 0.7 MPa
Stress (Pa)
Static Strain %

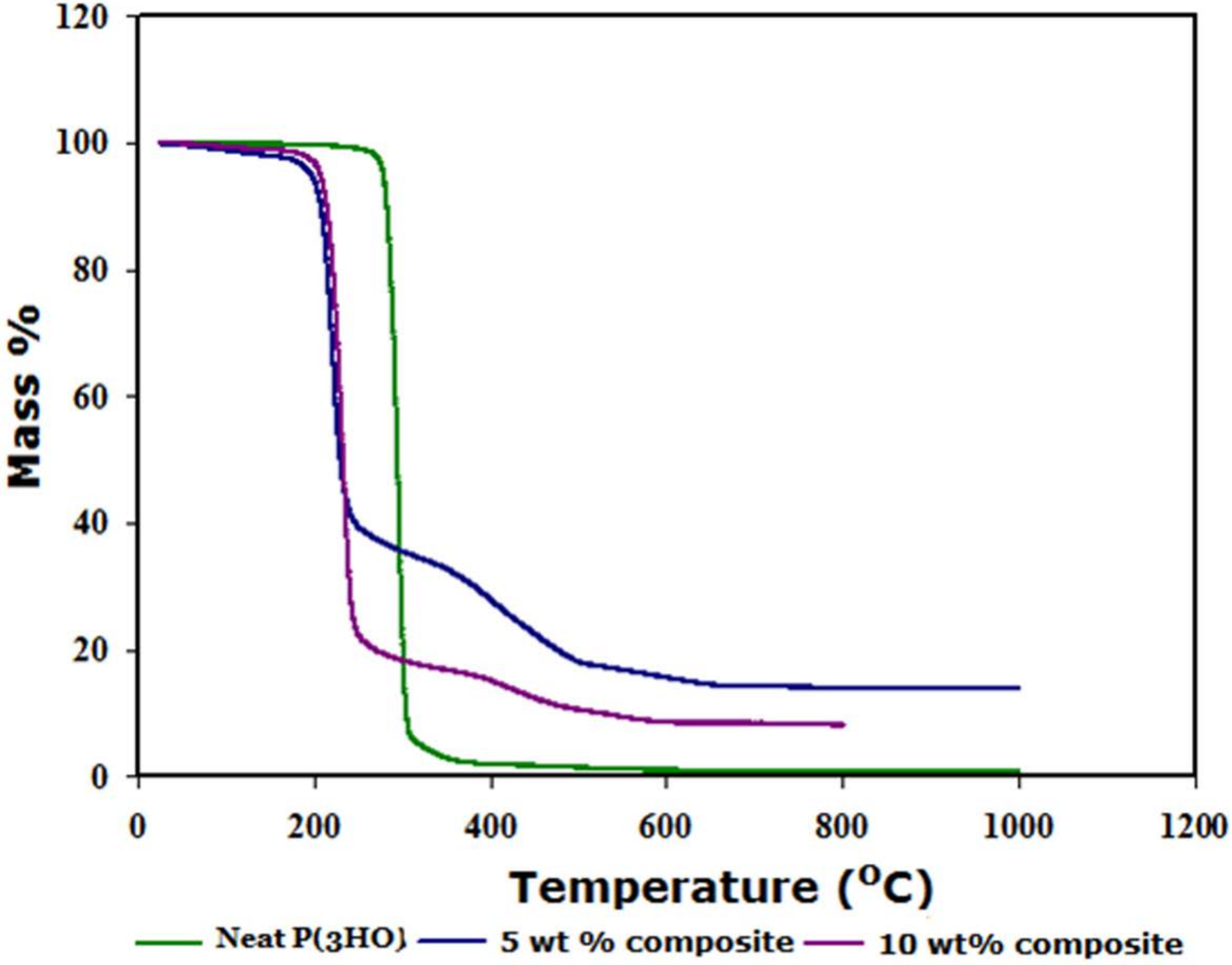
120
100
80
60
40
20
0
Mass %
0
200
400
600
800
1000
1200
Temperature (°C)
Neat P(3HO)
5 wt % composite
10 wt% composite